DOI: 10.6060/mhc245886z

Electronic and Steric Effects of Peripheral Substituents Impacting the Coordination and Redox Properties of Cobalt(III) Porphyrinates

Svetlana V. Zaitseva,[@] Sergey A. Zdanovich, Elena Yu. Tyulyaeva,[@] Aleksey N. Kiselev, and Sergey A. Syrbu

G. A. Krestov Institute of Solution Chemistry of the Russian Academy of Sciences, 153045 Ivanovo, Russian Federation
[@]E-mail: svz@isc-ras.ru, teu@isc-ras.ru

The coordinating ability of mixed-substituted cobalt(III) porphyrinates towards some N-bases was studied using spectrophotometric method. The regularities of the cooperative influence of electronic and steric effects of substituents at periphery of the macrocycle on the complexes' stability were established. The dependence of thermodynamic of coordination process on the N-base nature was studied. For initial cobalt(III) porphyrinates the calculated energy of frontier molecular orbitals, HOMO−LUMO gaps couple and the obtained electrochemical characteristics demonstrate the complexes to be able to participate in redox reactions.

Keywords: Porphyrin, cobalt complexes, phosphoryl and methoxy substituents, N-bases, distortion, reactivity.

Электронные и стерические эффекты периферических заместителей, влияющие на координационные и окислительно-восстановительные свойства порфиринатов кобальта(III)

С. В. Зайцева,[@] С. А. Зданович, Е. Ю. Тюляева,[@] А. Н. Киселев, С. А. Сырбу

Институт химии растворов имени Г.А. Крестова РАН, 153045 Иваново, Российская Федерация
[@]E-mail: svz@isc-ras.ru, teu@isc-ras.ru

Координационная способность смешаннозамещенных порфиринатов кобальта(III) по отношению к некоторым N-основаниям изучена спектрофотометрическим методом. Установлены закономерности совместного влияния электронного и стерического эффектов заместителей на периферии макроцикла на устойчивость комплексов. Изучена зависимость термодинамики процесса координации от природы N-основания. Рассчитанные для исходных порфиринатов кобальта(III) энергии граничных молекулярных орбиталей, величины зазора ВЗМО-НСМО и полученные электрохимические характеристики демонстрируют способность комплексов участвовать в окислительно-восстановительных реакциях.

Ключевые слова: Порфирин, комплексы кобальта, фосфорильные и метокси-заместители, N-основания, искажение, реакционная способность.

Introduction

The prosthetic group of heme-containing proteins such as cytochrome P450, heme peroxidases and heme catalases use the metalloporphyrin framework provided by the nature, as a starting point for the modelling the active sites of synthetic enzymes to create new generation catalysts of great applying prospect. Despite some features of the processes with enzymes participation, the key stages of the catalytic mechanism for many of them are very similar and involve the generation of a high-oxidized oxo-ferryl active species as a key intermediate.[1-3] The main question is about the basis of such multifunctionality of the highly efficient intermediate which is capable of stereo- and regio-specific oxidizing various substrates including aromatic rings and heterocycles, participating in the C–H bond acti-

vation and the C–C bonds cleavage in hydroxylation, dealkylation, epoxidation. In view of the nature-inspired interest to solute this question synthetic metalloporphyrins and their analogues are bound to become a hot biomimetic research topic.

Chemical facets of modeling go beyond the simple structural similarity of potential biomimetics with natural prosthetic groups. The features of the structure and properties of these molecular systems, ways to tune their activity are of paramount importance. One of the tools for such tuning is changing the composition through axial coordination. The ability of metalloporphyrin to coordinate both the small molecules and the high-molecular compounds plays the key role in the chemical and photochemical redox processes and defines the importance of non-covalent binding in ensuring the functioning of biosystems, catalysis, supramolecular chemistry,[4-8] creating the receptors, including molecular tweezers,[9-11] design the information storage and photoelectric devices.[12,13]

Proteins in the prosthetic group and peripheral substituents of the macrocycle are well-known to affect planarity and electronic state of porphyrin. Since distortions of the porphyrin ring are energetically unfavorable, enzyme activity may depend on the electronic and steric state of the metalloporphyrin. Thus, varying nonplanarity due to the effects of peripheral substituents can be used to tune the properties of biomimetics.

The fundamental insights gained from systematic studies of the coordination and redox properties of metalloporphyrins, depending on the nature of the macrocycle, substrate and metal atom may allow us to understand the mechanism of enzymes activation, find the ways to initiate the generation of highly oxidized intermediates of various types and control their reactivity.

This work focusses on the coordinating ability and redox properties of cobalt(III) porphyrinates (**1-4**), bearing peripheral substituents of the different electronic and steric effects and phosphoryl as an axial ligand (Scheme 1), studied using spectroscopy and electrochemistry techniques.

Experimental

Materials and synthesis

All N-bases were obtained from Sigma–Aldrich and used without purification unless indicated. The solvents were dried and distilled according to the published procedures. Cobalt porphyrinates (**1-4**) were synthesised following a previously published procedure.[14]

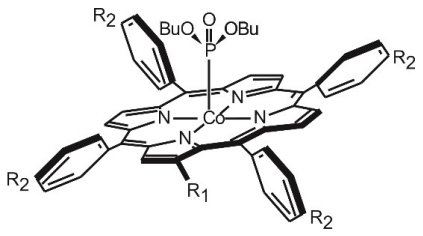

1 R_1, R_2 = H
2 R_1 = H, R_2 = *para*-OMe
3 R_1 = $PO(OBu)_2$, R_2 = H
4 R_1 = $PO(OBu)_2$, R_2 = *para*-OMe

Scheme 1.

*(5,10,15,20-Tetraphenylporphyrinato)cobalt(III) di-n-butoxyphosphite (**1**).* ^{1}H NMR ($CDCl_3$) δ ppm: 8.88 (8H, s, Hβ) 7.72 (12H protons of the phenyl rings, m), 8.11 (8H protons of the phenyl rings, m), 4.07 (4H, q, CH_2), 1.68 (4H, qv, CH_2), 1.44 (4H, sc, CH_2), 0.93 (6H, t, CH_3). IR (neat) ν_{max} cm^{-1}: 3735(w), 3436(s), 2923(w), 2850(w), 1625(m), 1438(w), 1405(w), 1384(m), 1348(w), 1200 (w), 1172(w), 1130(w) 1035(w), 1005 (w), 879 (w), 832 (w), 790(w), 752 (w), 689(w), 603 (w), 572 (w), 503 (w), 453(w), 417 (w). UV-Vis (DCM) λ_{max} nm (log ε): 409(5.17); 528(4.19); 558(3.81). HRMS (MALDI TOF) *m/z*: calculated for $C_{52}H_{46}CoN_4O_3P$: 864.26; determined experimentally: 864.23 $[M]^+$.

*(5,10,15,20-Tetrakis(4'-methoxyphenyl)porphyrinato)cobalt(III) di-n-butoxyphosphite (**2**).* ^{1}H NMR ($CDCl_3$) δ ppm: 10.23 (8H, s, Hβ), 8.07 (8H protons of the phenyl rings, d), 7.73-7.55 (12H protons of the phenyl rings, m), 4.33 (4H, t); 3.98 (4H, t); 5.32, (12H, s, CH_3), 1.59 (8H, bs, CH_2), 1.28 (8H, m, CH_2), 0.89 (12H, t, CH_3). IR (neat) ν_{max} cm^{-1}: 3893(w), 3847(w), 3770(w), 3727(w), 3660(w), 3419(s), 2954(w), 2921(m), 2854(w), 1612(m), 1508 (w), 1456 (w), 1384 (w), 1351(m), 1290 (w), 1245(w), 1174(w), 1124(w), 1029(w), 1000 (w), 890(w), 813 (w), 774(w), 719(w), 638 (w), 544 (w), 468(w), 412(w). UV-Vis (DCM) λ_{max} nm (log ε): 414(4.45); 531(3.66); 561(3.45). HRMS (MALDI TOF) *m/z*: calculated for $C_{56}H_{54}CoN_4O_7P$: 984.31; determined experimentally: 984.29 $[M]^+$.

*([2-(Di-n-butoxyphosphoryl)]-5,10,15,20-tetraphenylporphyrinato)cobalt(III) di-n-butoxyphosphite (**3**).* ^{1}H NMR ($CDCl_3$) δ ppm: 9.43 (1H, d, Hβ) 8.84 (3H, m, Hβ), 8.82 (1H, d, Hβ), 8.74 (1H, d, Hβ), 8.67 (1H, d, Hβ), 8.09 (8H protons of the phenyl rings, m), 7.71 (12H protons of the phenyl rings, m), 4.01 (4H, m), 1.66 (4H, qv), 1.39 (4H, m), 1.19 (2H, m), 0.96 (6H, m), 0.72 (2H, m), 0.42 (6H, m), 0.36 (4H, m), 0.17 (4H, m). IR (neat) ν_{max} cm^{-1}: 3729(w), 3450(s), 3417(s), 2960(w), 2925(w), 2856(w), 2401(w), 2266(m), 1716(w), 1670(w), 1592(w), 1461(w), 1390(w), 1345 (w), 1220(w), 1176(w), 1128(w), 1033(w), 1008(w), 827(w), 738(w), 675(w), 628(w), 588(w), 461(w). UV-Vis (DCM) λ_{max} nm (log ε): 414(5.13); 535(4.24); 569(4.02). HRMS (MALDI TOF) *m/z*: calculated for $C_{60}H_{63}CoN_4O_6P_2$: 1056.35; determined experimentally: 1056.37 $[M]^+$.

*([2-(Di-n-butoxyphosphoryl)]-5,10,15,20-tetrakis(4'-methoxyphenyl)porphyrinato)cobalt(III) di-n-butoxyphosphite (**4**).* ^{1}H NMR ($CDCl_3$) δ ppm: 10.21 (1H, s, Hβ), 8.21 (3H, m, Hβ), 7.98 (1H, d, Hβ), 7.90 (1H, d, Hβ), 7.73 (1H, m, Hβ), 8.07 (8H protons of the phenyl rings, d), 7.73-7.55 (8H protons of the phenyl rings, m), 4.33 (4H, t); 3.98 (4H, t); 5.32 (12 H, s, CH_3), 1.59 (8H, bs, CH_2), 1.28 (8H, m, CH_2), 0.89 (12H, t, CH_3). IR (neat) ν_{max} cm^{-1}: 3934(w), 3866(w), 3814(w), 3787(w), 3758(w), 3712(w), 3664(w), 3473(s), 3467(s), 3454(s), 3415(s), 3039(w), 2954(w) 2919(m), 2852 (w), 2595 (w), 2516 (w), 2439(w), 2335 (w), 2032(w), 1635 (m), 1614 (m), 1540 (w), 1508 (w), 1461(w), 1382(w), 1349(w), 1247(w), 1173(w), 1064(w), 1022(w), 908(w), 812(w), 720(w), 670 (w), 624(w), 538 (w), 471 (w), 432(w), 405(w); UV-Vis (DCM) λ_{max} nm (log ε): 420(4.86); 536(4.04); 570(3.85). HRMS (MALDI TOF) *m/z*: calculated for $C_{64}H_{71}CoN_4O_{10}P_2$: 1176.40; determined experimentally: 1176.41 $[M]^+$.

Spectroscopy

The UV-visible and mass-spectra were measured on Cary 50 UV-visible spectrophotometers at T=295 K and MALDI TOF Mass Spectrometer Shimadzu Axima Confidence, respectively.

ATIR-IR spectra were obtained on Bruker Vertex V80 in the frequency range 4000–400 cm^{-1} (64 scans on the average) with the resolution 2 cm^{-1} at the standard temperature. All IR spectra were recorded on a diamond crystal using a MVP 2 SeriesTM (Harrick) unit.

^{1}H NMR experiment was performed on a Bruker Avance III-500 NMR spectrometer.

Methods

The formation of N-base-ligated complexes in the acetonitrile was performed by titration experiments.

Equilibrium constants of complexformation were determined according to Equilibria (1, 2), based on the law of mass action and Bouguer–Lambert–Beer law, the latter being applied to two colored substances [15, 16]:

$$K_{eq} = [(L)_nMP]/[MP][L]^n \quad (1)$$

$$K_{eq} = \frac{\frac{A_w - A_o}{A_\infty - A_o}}{\frac{A_\infty - A_w}{A_\infty - A_o}} \cdot \frac{1}{c_L^\circ - c_{MP}^\circ \left(1 - \frac{A_w - A_o}{A_\infty - A_o}\right)} \quad (2)$$

In this equation A_0, A_w, A_∞ are optical densities of the MP solution, of the equilibrium mixture at certain concentration of N-base, and of the final coordination product, respectively; n was the number of the coordinated N-base molecules.

Organic bases were chosen owing to they are included in the composition of antibacterial, antitumor, anti-ischemic and antiallergic drugs.[17,18] N-bases are well-known to be easily coordinated by transition metal ions. Their presence as axial ligands in the coordination sphere of macrocyclic complexes can significantly affect the biological and catalytic activity of the resulted molecular complex as a whole.[19–22]

Theoretical calculations

All the DFT calculations for the current problem were performed using the Gaussian 09 W suite.[23] The B3LYP functionals were used to describe electron exchange and correlation,[24] while the 6-31g basis set was used to find the optimized geometries of reactants, products. The energy levels and the localization of the highest occupied molecular orbital (HOMO) and the lowest unoccupied molecular orbital (LUMO) of the studied compounds were determined by using minimized geometries to approximate the ground state.

Standard out-of-4N-plane deviations from planarity for the core atoms of the studied compounds were calculated using Microsoft Excel software.

Electrochemistry

Electrochemical measurements were performed by the cyclic voltammetry (CV) method with using a Potentiostat Biologic SP-150 according to procedure described elsewhere.[25] The CV response was recorded at scan rate 0.02 V/s. The CV data were corrected for Ohmic (iR) losses using the current interruption technique. The experiments were carried out in a three-electrode temperature-controlled (25 ± 0.5°C) electrochemical cell in freshly prepared solutions. As working electrode, we used a polishing Au strip (Dropsens DRP-C220AT) rigidly fixed in the fluoroplastic lid. The active surface of the working electrode was carefully cleaned in distilled water before every measurement and then in the solution under study. Working electrode was immersed in the cell with the test solution where the potential of the working electrode reached a steady value in 10 min. Argon was bubbled through the capillary tube for 30 min in order to deoxygenate solutions before the electrochemical measurements. Deoxygenation process was performed to avoid a superoxo-anion-radical formation $O_2 + \bar{e} \rightarrow O_2^{\bullet-}$.[26]

Tetrabutylammonium perchlorate (TBAP ≥ 98.0, ALDRICH) was purified by recrystallization from ethanol. Solution of the examined compound (C = 0.1 mM) contains 0.02 M TBAP as the supporting electrolyte.

Results and Discussion

The reversible bonding of nitrogen-containing ligands such as imidazole (Im), 1-methylimidazole (1-MeIm), 2-methylimidazole (2-MeIm), benzimidazole (BzIm) pyridine (Py), bipyridine (BiPy) and pyrazine (Prz) with cobalt(III) porphyrinates (**1**–**4**) was studied applying a spectrophotometric titration in wide concentration region in acetonitrile at 295K ($C_{1\text{-MeIm}}$ = 6.5·10^{-5}–1.2·10^{-2} M, C_{Im} = 9.5·10^{-5}–1.5·10^{-2} M, $C_{2\text{-MeIm}}$ = 1.2·10^{-4}–2.4·10^{-2} M, C_{BzIm} = 2.5·10^{-4}–4.9·10^{-2} M, C_{Py}= 2.7·10^{-4}–5.2·10^{-2} M, C_{BiPy} = 3.07·10^{-4}–6.1·10^{-2} M, C_{Prz} = 2.4·10^{-3}–6.9·10^{-1} M). The evaluation of coordinating ability of the studied complexes is described using compound **4** as an example (Figures 1). For all the compounds ligation resulted in red shifts of B- and Q-bands (Figure 1). The shift values are affected by the nature of substituents and the substrates (Table 1). The well-defined isosbestic points indicated that during the course of the experiment, additional intermediates do not accumulate in spectroscopically significant concentrations.

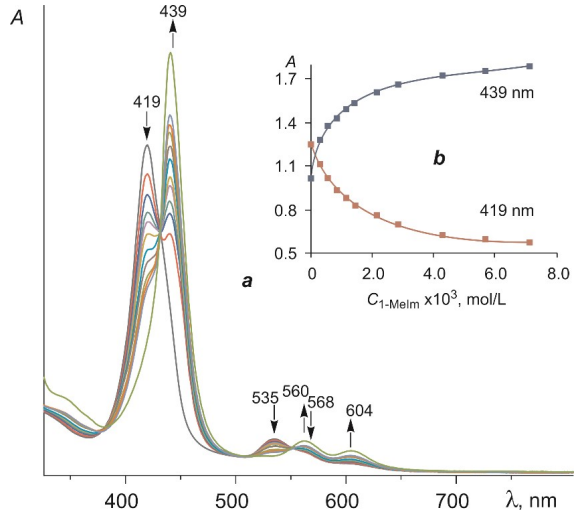

Figure 1. UV-visible spectra of complex **4** (C = 5.60·10^{-6} M) with additions of 1-MeIm ($C_{1\text{-MeIm}}$ = 0–1.10·10^{-2} M) in acetonitrile (CH_3CN). Inserts: corresponding titration curves at λ_{max} =419, 439 nm.

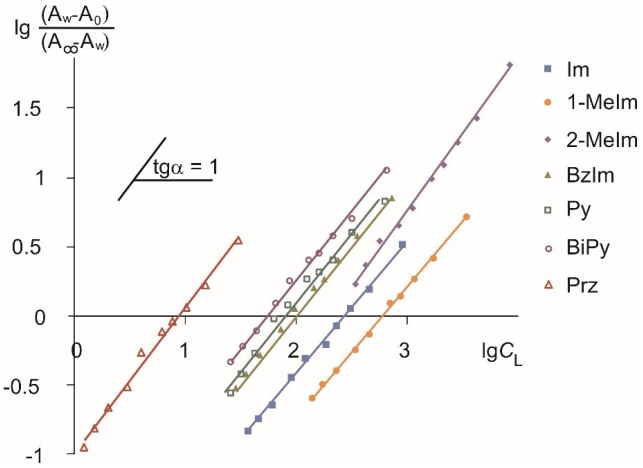

Figure 2. Dependence lg(A_w – A_0)/(A_∞ – A_w)=f lgC_L for the reactions of complexes **4** with N-bases in acetonitrile 298 K (R^2 = 0.9703–0.9917).

Table 1. The B- and Q-bands in UV-visible spectra (λ_{max}, nm, CH_3CN) and characteristic vibration frequency in IR spectra (ν, cm^{-1}) for compounds **1-4** and their N-base-liganded complexes.

Complex	λ_{max}, nm (CH_3CN)	$\Delta\lambda_B$	ν(P=O), cm^{-1}	ν(Co-Np)/ (Co-N_{Im}), cm^{-1}
1	558, 528, 409 [a] 556, 528, 407		1200	453
1+1-MeIm	599, 558, 434	27		
1+Im	597, 556, 432	25	1227	439/430
1+2-MeIm	593, 554, 428	21		
1+BzIm	590, 552, 426	19		
1+Py	590, 553, 423	16		
1+BiPy	588, 552, 420	13		
1+Prz	573, 544, 415	8		
2	561, 531, 414 [a] 559, 529, 413		1245	468
2+1-MeIm	601, 559, 437	24		
2+Im	596, 557, 435	22	1263	444/426
2+2-MeIm	591, 554, 431	18		
2+BzIm	588, 550, 429	16		
2+Py	585, 548, 427	14		
2+BiPy	586, 546, 426	13		
2+Prz	577, 540, 419	6		
3	569, 535, 415 [a] 566, 533, 414		1220	461
3+1-MeIm	587, 557, 436	22		
3+Im	585, 550, 433	19	1240	447/423
3+2-MeIm	581, 548, 429	15		
3+BzIm	580, 546, 427	13		
3+Py	578, 545, 426	11		
3+BiPy	577, 542, 423	9		
3+Prz	573, 538, 419	5		
4	570, 536, 421 [a] 568, 535, 419		1247	471
4+1-MeIm	604, 560, 439	20		
4+Im	587, 552, 435	16	1261	445/421
4+2-MeIm	584, 550, 432	13		
4+BzIm	580, 548, 429	10		
4+Py	578, 546, 428	9		
4+BiPy	576, 544, 426	7		
4+Prz	574, 540, 423	4		

[a] in CH_2Cl_2

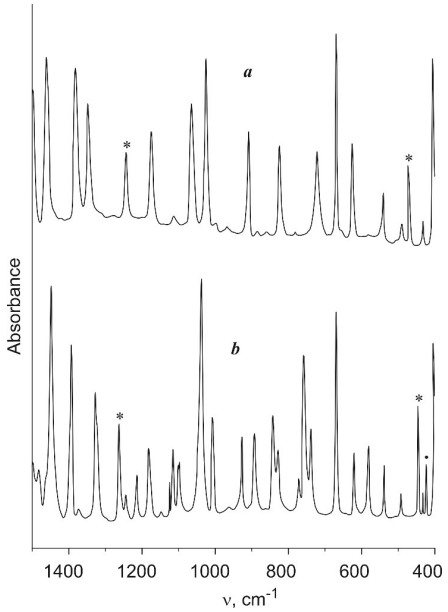

Figure 3. IR spectra (in KBr) of complexes **4** (a) and **4**-Im (b) (C_4= 5.56·10^{-6} M, C_{Im}= 6.18·10^{-3} M). • ν(Co–N_L); * ν(Co–Np), ν(P=O).

The degree of substrate specificity of any complex significantly depends on the implementation of coordination interactions in the receptor-substrate system and is defined by composition and stability of resulting axial complex. To determine the composition of the liganded complex, spectrophotometric titration methods are applied, namely the molar ratio method and the limited logarithmic method.[20-28] The composition of the axial complex in our work was determined from the slope of the linear dependence the $\lg(A_\tau - A_0)/(A_\infty - A_\tau) = f\lg C_L$. Complexes **1**–**4** were found to bond one molecule of N-base in all the experiments (Figure 2).

The complexation between the initial compounds and nitrogen-containing bases was confirmed by IR and mass spectra. Fist, along with unchanged vibrations of macrocycles in the region 350–1500 cm^{-1} IR spectra demonstrated essential shift of the band of vibrations ν(P=O) assignable to cobalt porphyrinates (**1**–**4**).[14] For example, in the case of ligation of complex **4** with Im this band at ν = 1247cm^{-1} in the IR spectrum was high-frequency shifted by 14 cm^{-1}. Next, the signals ν = 471 cm^{-1} attributable to the ν(Co–Np) were shifted by 26 cm^{-1} to the low-frequency region of the

spectrum (Figure. 3). Additionally, a new band assigned to Co–N_{Im} bond appeared at 421 cm^{-1}. The observed shifts of the characteristic vibrations ν(P=O) and ν(Co–Np) indicate the displacement of the cobalt atom relative to the coordination plane N4 caused by the formation of the cobalt-substrate bond. For complexes **1**-Im, **2**-Im and **4**-Im the characteristic frequencies are listed in Table. 1.

A MALDI TOF mass spectrum of complex **4** after reaction with Im in CH_3CN showed dominating signal at *m/z* = = 1056.46 due to $[\mathbf{4}]^+$ together with an ion cluster at *m/e* = = 1124.42 attributable to ion $[\mathbf{4}+Im]^+$ (Figure 4). The interaction of complexes **1-3** and imidazole was also evidenced by mass spectrometry.

The results in Table 2 show the equilibrium constants for the axial complexes of 1:1 composition to correlate with the substrates basicity value (pK_a)[29] in the following order Prz<BiPy< Py < BzIm < 2-MeIm <Im<1-MeIm. Linearity is disrupted in the cases of BiPy, BzIm and 2-MeIm, when bases enhance the steric hindrance during coordination (Figure 5).

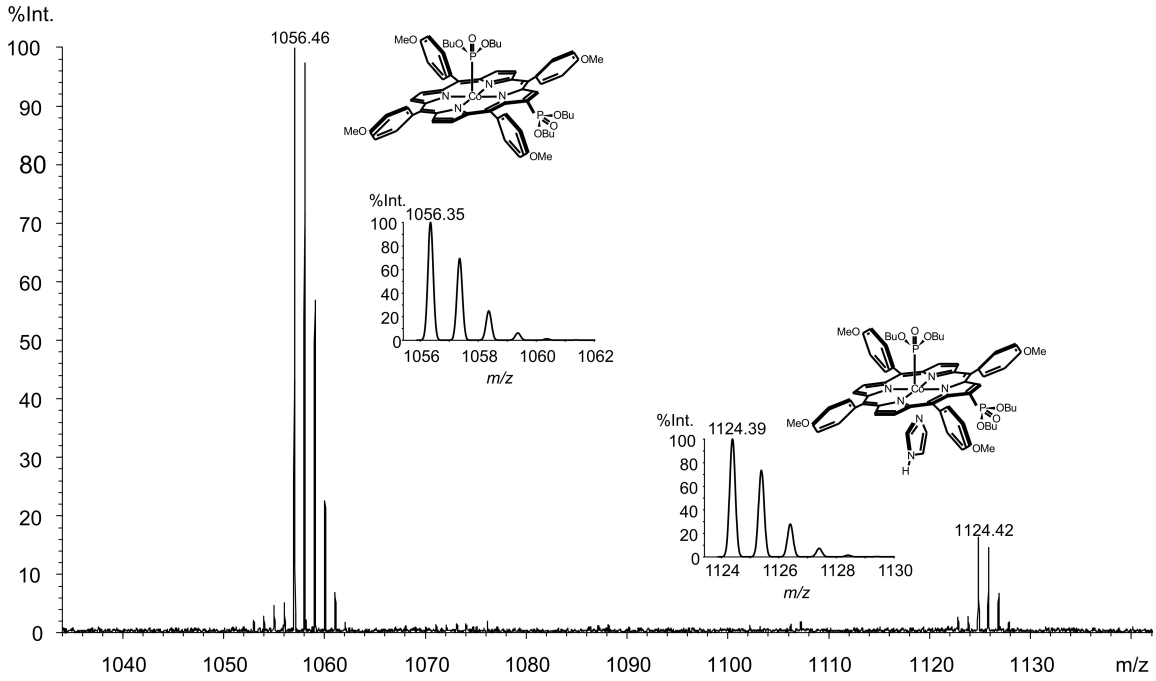

Figure 4. MALDI TOF spectra of the complexes **4** (C_4= 5.6·10^{-6} M) after reaction with Im (C_{Im} = 6.2·10^{-3} M). Solvent: CH_3CN.

Table 2. The equilibrium constants (lgK_s^{298}) for the axial complexes of cobalt porphyrinates **1-4** and pK_a values of N-bases.

Complex	N-base	pK_a	lgK_s^{298}
1	1-MeIm	7.33	3.47
	Im	6.95	3.38
	2-MeIm	5.89	3.14
	BzIm	5.53	2.88
	Py	5.29	2.73
	BiPy	4.82	2.55
	Prz	0.6	1.35
2	1-MeIm	7.33	3.34
	Im	6.95	3.25
	2-MeIm	5.89	2.95
	BzIm	5.53	2.7
	Py	5.29	2.64
	BiPy	4.82	2.42
	Prz	0.6	1.24
3	1-MeIm	7.33	3.29
	Im	6.95	2.96
	2-MeIm	5.89	2.76
	BzIm	5.53	2.45
	Py	5.29	2.41
	BiPy	4.82	2.28
	Prz	0.6	1.12
4	1-MeIm	7.33	2.78
	Im	6.95	2.43
	2-MeIm	5.89	2.26
	BzIm	5.53	1.97
	Py	5.29	1.90
	BiPy	4.82	1.75
	Prz	0.6	0.95

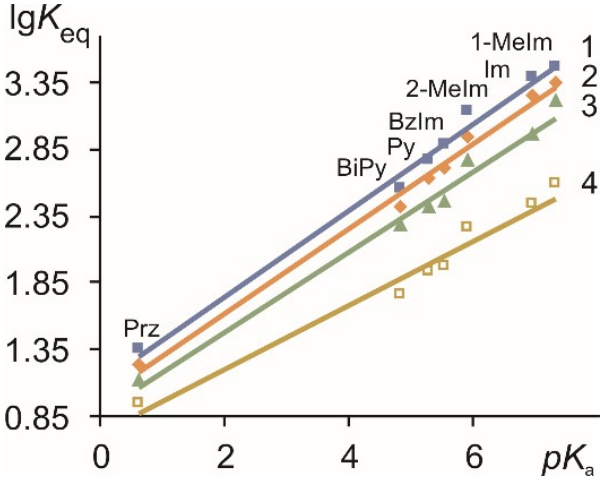

Figure 5. Dependence of the equilibrium constants (lgK_{eq}) on substrates basicity value (pK_a) for axial complexes of cobalt porphyrinates **1**–**4.**

Following data obtained (Table 2) the stability of axial complexes decreases in the order **1** > **2** ≥ **3** > **4**. The resulting trend can be reasonable explained by the electronic and steric effects of substituents in the macrocycle. A stronger receptor-substrate bonding is known to occur in the case of more electron-deficient porphyrin ligand, which is capable of increasing the effective positive charge on the metal atom. The presence of electron-withdrawing phosphoryl and electron-donating methoxy groups may either decreases or increases the basicity of the porphyrin ligand. When the complexes are mixed-substituted effect can be expected to be mutual. In the cases of the compounds under investigation, phosphoryl groups are located in the coordination unit (as acidoligand) or in the β-position of the pyrrole. Therefore, their influence on the porphyrin π-system is more than that of *para*-methoxyl groups in phenyls.[30-32] It is clearly that the more significant electron-withdrawing effect can only be slightly compensated by the electron-donating groups. In this case, compound **3** should be expected to be superior in coordinating ability to other cobalt porphyrinates but evidence does not back this up.

On the other hand, the presence of bulky acidoligand and the insertion of functional groups into the β-positions of the pyrroles results in essential rise in the porphyrin ligand nonplanarity.[30-32] Enhancing steric distortion of the macrocycle leads to a decrease in its aromaticity. As a result, the porphyrin ligand becomes more basic and diminish the ability to bind the substrates compare to the complexes bearing electron-deficient substituents.

To estimate the degree of nonplanarity of the macrocycles, we used the standard deviation (σ) of the skeletal atoms from the average plane of the porphyrin molecule, calculated by the DFT method.[23,24] Geometry optimization was carried out for complexes **1-4** in the singlet spin state.

As Figure 6 shows the sequential increase in the number of phosphoryl functional groups at the axial and β-positions of the macrocycle turns out to distort the molecules sharply. The non-planar conformations of porphyrin ligands are owing to tilting of the pyrrole rings as a result of push and pull effects between substituents. Such interactions elongate C_β–C_β bonds and increase the C_β–C_α–C_m and N–C_α–C_m bond angles, compared to unsubstituted (OH)CoTPP (Table 3). While complexes **1** and **2** are dominated by corrugated deformation, complexes **3** and **4** exhibit nonplanar conformational distortions in the shape of a saddle (Figure 6) with varying degrees of nonplanarity of the optimized molecules according the values of Δ24 and σ (Table 3). Thus, in the case of complexes under study the combination of two phosphoryl groups in close proximity to the coordination center, with methoxy substituents in the phenyl fragments is accompanied by an increase in nonplanarity in the following order **1** < **2** < **3** < **4** (Figure 6, Table 3). The standard deviation values (σ) are in good agreement with experimental data on the stability of axial complexes. The lower the degree of nonplanarity of the initial compound (σ value), the stronger the metal-N-base bonding in the resulted complex (Tables 2, 3, Figure 7).

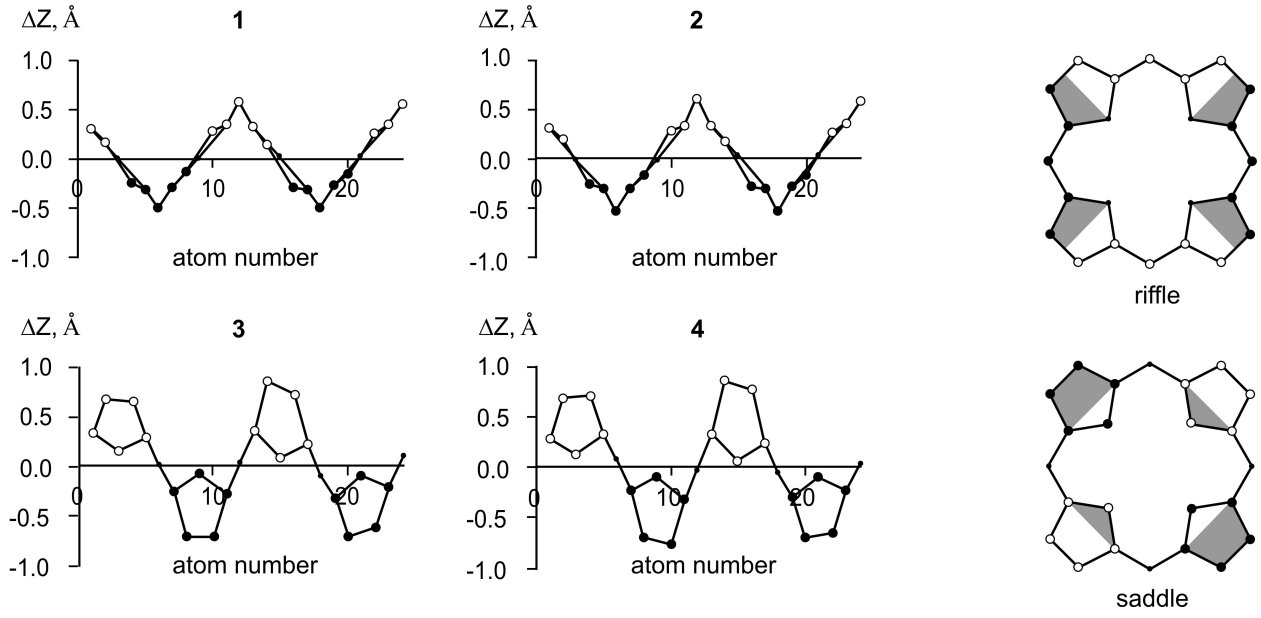

Figure 6. Linear display of the out-of-N4 plane deviations from planarity for the core atoms of the studied compounds.

Table 3. Selected geometrical data for complexes **1-4** and corresponding deviations of the skeletal atoms from the average plane.

Complex	$C_{\beta 17}$–$C_{\beta 18}$, Å	$C_{\beta 18}$–$C_{\alpha 19}$–C_m/ N–$C_{\alpha 19}$–C_m $C_{\beta 17}$–$C_{\alpha 16}$–C_m/ N–$C_{\alpha 16}$–C_m, °	Δ24, Å	σ
1	1.365	124.05/125.50 124.84/125.17	0.2648	0.3097
2	1.367	124.79/125.25 124.00/125.57	0.2653	0.3186
3	1.372	124.37/125.49 127.11/123.17	0.3504	0.4383
4	1.380	125.52/125.30 128.38/124.64	0.3589	0.4524
(OH)CoTPP	1.360	123.88/125.66 123.91/125.87	0.2282	0.2619

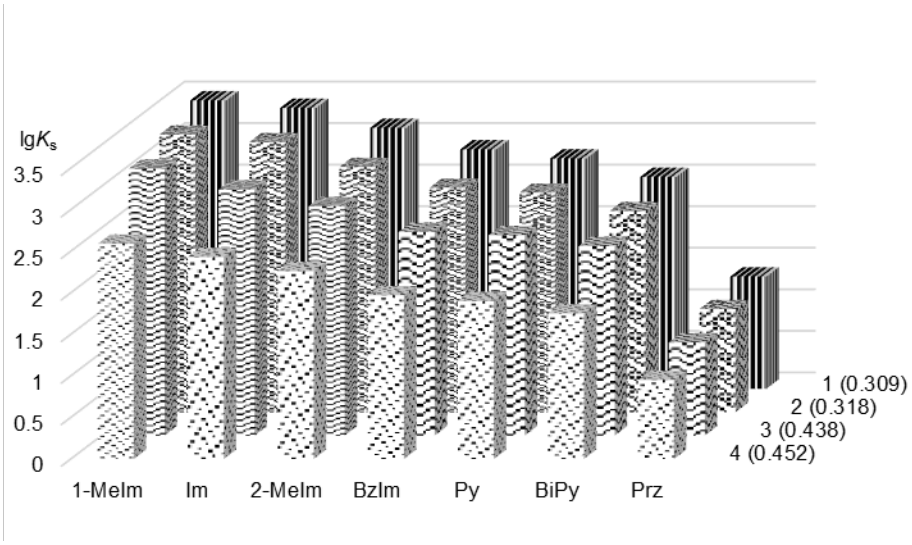

Figure 7. Dependence of stability of the axial complexes of cobalt porphyrinates **1-4** on the macrocycle nonplanarity degree (indicated in brackets).

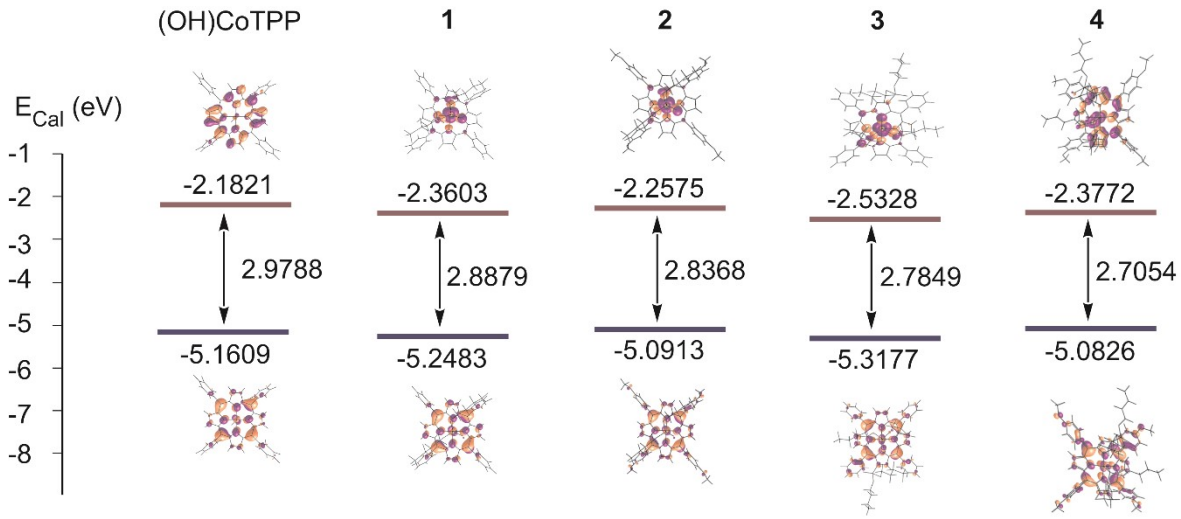

Figure 8. The molecular orbitals energy (eV) and the HOMO−LUMO gaps (ΔE_g) of the studied cobalt porphyrinates.

The additional information on the correlation between structure and properties of the examined compounds can be obtained applying theoretical calculation of geometric and energy parameters, namely the relative energy position and shape of the HOMO and LUMO frontier molecular orbitals and HOMO−LUMO gaps of studied compounds, coupled with spectral studies. Simulating the compounds is known to ensure estimation of their stability and reactivity including in redox reactions, since an electron transfer feasibility depends on E_{HOMO}, E_{LUMO} and ΔE_g values.

The theoretical calculations were performed for complexes **1-4**. The selected DFT-predicted HOMOs, LUMOs of all the studied compounds are listed in Table 3. HOMOs are certain to be mainly located on porphyrin rings especially on C_α-atoms of the porphyrin core with the extent of delocalization appears to decrease when changing from **1** to

4 (Figure 8). The electronic density which is not spread over the porphyrin structures seems to determine distortion of the studied compounds.

For all the complexes the HOMO and HOMO-1 energy are similar to each other (0.052-0.106 eV). As the orbitals are porphyrin-centered the abstraction of the first and second electron must occur from the macrocyclic ligand and the most reactive in oxidation should be complex **4** according to the minimum ΔE_g value among examined cobalt porphyrinates (Figure. 8). Decreasing ΔE_g value in order **1 > 2 > 3 > 4** is in the excellent agreement with the rise in the conformational distortions of the macrocycles (Figure 6, Table 3) and destabilization of the FMOs as well as with experimentally obtained stability of molecular N-base-liganded complexes of cobalt porphyrinates.

Additionally, the oxidation capacity of the initial compounds was estimated. The electrochemical behaviour of compounds **1-4** in solutions was investigated using cyclic voltammetry in dichloromethane, using Bu_4NPF_6 as the supporting electrolyte at room temperature (Table 4, Figure 9). The compounds underwent two successive reversible oxidations attributable to two sequential one-electron oxidations of the macrocycle resulting in π-cation-radical and di-cation species.

Table 4. Oxidation potentials of cobalt porphyrinates under study in CH_2Cl_2 (*vs*. Ag/AgCl) and previously published data for some compounds.

Complex	E_{ox}, V	
	0/+	+/2+
1	0.95	1.20
2	0.80	1.06
3	0.88	1.14
4	0.78	1.03
Zn(5,15-(4'-$MeO_2CC_6H_4$))-(10-$PO(OEt)_2$)P[33]	0.99	1.21
Zn(5,15-$P(O)(OEt)_2$)-(10,20-$(Ph)_2$)P[34]	1.06	1.32
Cu(5,15-$P(O)(OEt)_2$)-(10,20-$(Ph)_2$)P[34]	1.22	1.36
ZnTPP[34]	0.83	1.18
CuTPP[34]	0.99	1.33
(Cl)CoTPP[35]	0.90	1.50

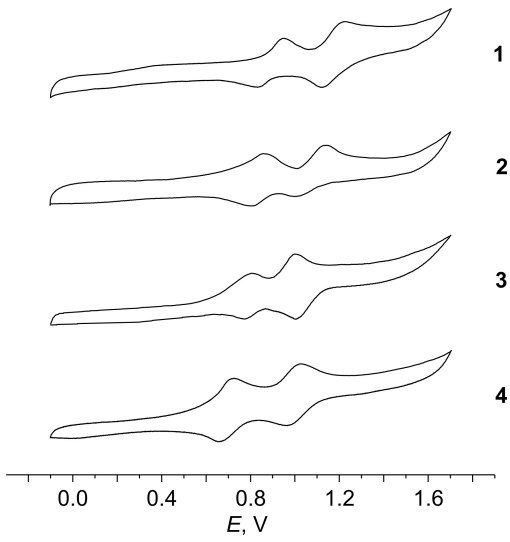

Figure 9. CV responses for complexes **1-4** in CH_2Cl_2 recorded at scan rate 0.02 V/s.

In accordance with electron-withdrawing effect of a group at β-position of the macrocycle, the highest oxidation potential would be expected for compound **3**. However, significant distortions in this compound cause growth in the basicity of the macrocycle (and, therefore, offset the electron-deficient influence of the substituent) resulting in the diminish in the first oxidation potential (Table 4). The change of the oxidation potentials for **1, 2, 4** appears to be due to combined electron-releasing/withdrawing electronic effect of the substituents and the nonplanarity magnitude of the macrocycle. Generally, electrochemical data confirm the highest and lowest stability in the oxidation reaction for complexes **1** and **4**, respectively, that is consistent with the above results.

Conclusions

In bringing together the findings on cobalt porphyrins **1-4**, this report intends to broaden our current understanding of the factors that control the stability and reactivity of the studied compounds toward N-bases and oxidants. The easy complexation with N-bases, the sharp spectral response to changes in the composition of the complex, moderate substrate specificity of the compounds, originating from both the electronic and steric effects of the substituents and the nature of the base, allow us to predict the feasibility of binding the biologically active molecules containing N-bases or their derivatives with such complexes. The results show both electronic and steric effects of substituents to be important for the coordinating ability tuning with the latter being decisive. The calculated energy of frontier molecular orbitals, HOMO−LUMO gaps, and the obtained electrochemical characteristics of the complexes demonstrate their ability to participate in redox reactions. Generally, this knowledge should, in turn, point toward new strategies for constructing biomimetic catalysts that rely on reactive intermediates.

Acknowledgements. This work was supported by the research planning "Tetrapyrrole macroheterocyclic compounds - the relationship between physicochemical and applied properties" (№ 122040500043-7). This work was carried out with the help of the centers of the scientific equipment collective use "The upper Volga region center of physicochemical research".

References

1. Huang X, Groves J.T. *Chem. Rev.* **2018**, *5*, 2491–2553. doi 10.1021/acs.chemrev.7b00373.
2. Poulos T.L. *Chem. Rev.* **2014**, *7*, 3919–3962.
3. Oszajca M., Franke A., Brindell M., Stochel G., van Eldik R. *Coord. Chem. Rev.* **2016**, *306*, 483–509. doi 10.1016/j.ccr.2015.01.013.
4. Kustov A.V. *ChemChemTech [Izv. Vyssh. Uchebn. Zaved. Khim. Khim. Tekhnol.]* **2023**, *12*, 32–40. doi 10.6060/ivkkt.20236612.6902.
5. Sanders J.K., Bampos N., Clyde-Watson Z., Darling S.L., Hawley J.C., Kim H.J., Mak C.C., Webb S.J. In: *Porphyrin Handbook, Vol. 3* (Kadish K.M., Smith K.M., Guilard R.), San Diego: Academic Press, **2000**, p. 1– 48.
6. Beletskaya I., Tyurin V.S., Tsivadze A.Yu., Guilard R., Stern C. *Chem. Rev.* **2009**, *5*, 1659–1713. doi 10.1021/cr800247a.

7. Vashurin A.S., Bobrov A.V., Botnar A.A., Bychkova A.N., Gornukhina O.V., Grechin O.V., Erzunov D.A., Kovanova M.A., Ksenofontova K.V., Kuznetsov V.V., Lefedova O.V., Latypova A.R., Litova N.A., Marfin Yu.S., Pukhovskaya S.G., Tarasyuk I.A., Tikhomirova T.V., Rumyantsev E.V., Usoltsev S.D., Filippov D.V. *ChemChemTech [Izv. Vyssh. Uchebn. Zaved. Khim. Khim. Tekhnol.]* **2023**, *7*, 76–97. doi 10.6060/ivkkt.20236607.6840j.
8. Znoyko S.A., Maizlish V.E., Koifman O.I. *ChemChemTech [Izv. Vyssh. Uchebn. Zaved. Khim. Khim. Tekhnol.]* **2024**, *1*, 6–35. doi 10.6060/ivkkt.20246701.6859.
9. Kim D., Lee S., Gao G., Kang H.S., Ko J. *J. Organomet. Chem.* **2010**, *1*, 111–119. doi 10.1016/j.jorganchem. 2009.09.035.
10. Vinodh M., Alipour F.H., Mohamod A.A., Al-Azemi T.F. *Molecules* **2012**, *17*, 11763–11799. doi 10.3390/ molecules171011763.
11. Hayashi T., Ogoshi H. *Chem. Soc. Rev.* **1997**, *26*, 355–364.
12. Maligaspe E., Tkachenko N.V., Subbaiyan N.K., Chitta R., Zandler M.E., Lemmetyinen H., D'Souza F. *J. Phys. Chem., A* **2009**, *30*, 8478–8489. doi 10.1021/jp9032194.
13. Skvortsov I.A., Chufarin A.E., Zaitsev M.V., Kirakosyan G.A., Stuzhin P.A. *Asian J. Org. Chem.* **2023**, *12*, e202300425. doi 10.1002/ajoc.202300425.
14. Kiselev A.N., Zaitseva S.V., Zdanovich S.A., Shagalov E.V., Aleksandriysky V.V., Syrbu S.A., Koifman O.I. *Chemistry Select* **2021**, *6*, 12188.
15. Bulatov M.I., Kalinkin I.P. *Practical Guide on Photocolorimetric and Spectrophotometric Methods*. Leningrad, **1986**. 432 p. [Булатов М.И., Калинкин И.П. *Практическое руководство по фотометрическим методам анализа.* Ленинград: Химия, 1986. 432 с.].
16. Zaitseva S.V., Zdanovich S.A., Tyulyaeva E.Y., Grishina E.S., Koifman O.I. *J. Porphyrins Phthalocyanines* **2016**, *5*, 639–646. doi 10.1142/S1088424616500474.
17. Khatami M.H., Bromberek M., Saika–Voivod I., Booth V. *Biochim. Biophys. Acta (BBA) – Biomembranes* **2014**, *11*, 2778–2787 doi 10.1016/j.bbamem.2014.07.013.
18. Blindauer C.A. *J. Inorg. Biochem.* **2008**, *3*, 507–521. doi 10.1016/j.jinorgbio.2007.10.032.
19. Praneeth V.K.K., Näther C., Peters G., Lehnert N. *Inorg. Chem.* **2006**, *7*, 2795–2811. doi 10.1021/ic050865j.
20. Zaitseva S.V., Zdanovich S.A., Koifman O.I. *Macroheterocycles* **2012**, *1*, 81–86. doi 10.6060/mhc2012.111149z.
21. Mamardashvili G.M., Mamardashvili N.Zh., Koifman O.I. *Macroheterocycles* **2013**, *6*, 67–73. doi 10.6060/ mhc130226m.
22. Zaitseva S.V., Zdanovich S.A., Kudrik E.V., Koifman O.I. *Russ. J. Inorg. Chem.* **2017**, *9*, 1257–1266. doi 10.1134/ s0036023617090194.
23. *Gaussian 09, Revision A.02,* Frisch M.J., Trucks G.W., Schlegel H.B., Scuseria G.E., Robb M.A., Cheeseman J.R., Scalmani G., Barone V., Petersson G.A., Nakatsuji H., Li X., Caricato M., Marenich A., Bloino J., Janesko B.G., Gomperts R., Mennucci B., Hratchian H.P., Ortiz J.V., Izmaylov A.F., Sonnenberg J.L., Williams-Young D., Ding F., Lipparini F., Egidi F., Goings J., Peng B., Petrone A., Henderson T., Ranasinghe D., Zakrzewski V.G., Gao J., Rega N., Zheng G., Liang W., Hada M., Ehara M., Toyota K., Fukuda R., Hasegawa J., Ishida M., Nakajima T., Honda Y., Kitao O., Nakai H., Vreven T., Throssell K., Montgomery J.A.,Jr., Peralta J.E., Ogliaro F., Bearpark M., Heyd J.J., Brothers E., Kudin K.N., Staroverov V.N., Keith T., Kobayashi R., Normand J., Raghavachari K., Rendell A., Burant J.C., Iyengar S.S., Tomasi J., Cossi M., Millam J.M., Klene M., Adamo C., Cammi R., Ochterski J.W., Martin R.L., Morokuma K., Farkas O., Foresman J.B., Fox D.J., Gaussian, Inc., Wallingford CT, **2016**.
24. Kuvshinova E.M., Bykova M.A., Vershinina I.A., Gornukhina O.V., Lyubimova T.V., Semeikin A.S. *ChemChemTech [Izv. Vyssh. Uchebn. Zaved. Khim. Khim. Tekhnol.]* **2018**, *7*, 44–49. doi 10.6060/ivkkt.20186107.5843.
25. Kuzmin S.M., Chulovskaya S.A., Parfenyuk V.I. *J. Porphyrins Phthalocyanines* **2014**, *18*, 585–593. doi 10.1142/ S108842461450031X.
26. Kuzmin S.M., Chulovskaya S.A., Parfenyuk V.I. *J. Porphyrins Phthalocyanines* **2015**, *19*, 1053–1062. doi 10.1142/ S1088424615500807.
27. Ye L., Fang Y., Ou Z., Wang L., Xue S., Lu Y., Kadish K.M. *J. Porphyrins Phthalocyanines* **2019**, *23*, 196–205. doi 10.1142/S1088424619500135.
28. Zaitseva S.V., Zdanovich S.A., Koifman O.I., Tyurin D.V. *Russ. J. Gen. Chem.* **2018**, *6*, 1142–1147. doi 10.1134/ S1070363218060166.
29. Sievertsen S., Murray K.S., Moubaraki B., Berry K.J., Korbatieh Y., Cashion J.D., Brown L.J., Homborg H. *ZAAC* **1994**, *7*, 1203–1212. doi 10.1002/zaac.19946200713.
30. Zaitseva S.V., Zdanovich S.A., Koifman O.I. *Russ. J. Gen. Chem.* **2013**, *4*, 738–743. doi 10.1134/S1070363213040221
31. Qiu D., Kumar M., Ragsdale S.W., Spiro T.G. *Science* **1994**, *5160*, 817–819. doi 10.1126/science.8171334.
32. Bhyrappa P., Arunkumar C., Varghese B. *Inorg. Chem.* **2009**, *9*, 3954–3965. doi 10.1039/C9DT00706G.
33. Nefedov S.E., Birin K.P., Bessmertnykh-Lemeune A., Enakieva Y.Y., Sinelshchikova A.A., Gorbunova Y.G., Tsivadze A.Y., Stern Ch., Fangd Y., Kadish K.M. *Dalton Trans.* **2019**, *16*, 5372–5383.
34. Paul-Roth C., Rault-Berthelot J., Simonneaux G., Poriel C., Abdalilah M., Letessier J. *J. Electroanalyt.l Chem.* **2006**, *1*, 19–27.
35. Kadish K.M., Lin X.Q., Han B.C. *Inorg. Chem.* **1987**, *25*, 4161–4167.

Received 19.04.2024
Accepted 04.10.2024